BALANCED EARTH SATELLITE ORBITS

V. KUDIELKA *
Peter Jordan Str. 165, A-1180 Vienna, Austria

(Received 9 November, 1993; accepted 28 July, 1994)

Abstract. An analytic model for third-body perturbations and for the second zonal harmonic of the central body's gravitational field is presented. A simplified version of this model applied to the Earth-Moon-Sun system indicates the existence of high-altitude and highly-inclined orbits with their apsides in the equator plane, for which the apsidal as well as the nodal motion ceases. For special positions of the node, secular changes of eccentricity and inclination disappear too ("balanced" orbits). For an ascending node at vernal equinox, the inclination of balanced orbits is 94.56°, for a node at autumnal equinox 85.44°, independent of the eccentricity of the orbit. For a node perpendicular to the equinox, there exist circular balanced orbits at 90° inclination. By slightly adjusting the initial inclination as suggested by the simplified model, orbits can be found – calculated by the full model or by different methods – that show only minor variations in eccentricity, inclination, argument of perigee, and longitude of the ascending node for 10^5 revolutions and more. Orbits near the unstable equilibria at 94.56° and 85.44° inclination show very long periodic librations and oscillations between retrogade and prograde motion.

Key words: Artificial satellite theory, luni-solar perturbations, near polar inclinations.

1. Introduction

As early as 1805 P.S. Laplace treated the problem of the gravitational effects of an oblate central body together with third body perturbations on circular satellite orbits – the moons of Jupiter and the rings and moons of Saturn.

With the advent of artificial satellites the interest in this field exploded. Luni-solar perturbations of Earth satellite orbits have been analysed by many authors, but sometimes without considering the oblateness of the Earth, for example, Lorell (1965), Roy (1969), or by treating luni-solar effects as of second order only, for example, Hough (1981). Hough made it very clear that "For semimajor axes between 3 and 6 Earth radii, ... Earth oblateness and lunisolar gravity must both be treated as first-order effects". General models including both effects have been published by Lidov (1961), Cook (1962), Shapiro (1962) and others. When looking for resonance effects, especially Cook (1962) and Hughes (1980) were very useful for the author's understanding of the long-periodic behaviour of satellites (OSCAR 10 and AO-13) in high-altitude orbits (semi-major axes around 4 Earth radii) at somewhat unusual inclinations (around 26 and 57 degrees), which are very near to 5 : 3 and 1 : 2 resonances of apsidal to nodal motion.

Almost all of today's highly-inclined, high-altitude orbits like Molniya, Tundra, M-HEO, etc., see, for example, Solari and Viola (1992), are positioned near the

* Retired from IBM Vienna Software Development Laboratory.

Celestial Mechanics and Dynamical Astronomy **60:** 455–470, 1994.

"critical" inclination of 63.43° and with an argument of perigee of around 270°, in order to serve primarily the northern hemisphere. These orbits are all very well researched. When looking for other orbits useful for world-wide communications, a general overview is still missing in the open literature.

The intention of this paper is to present:

(1) a complete model of third body perturbations affecting orbits around an oblate central body, following Cook's approach (1962), and

(2) a few unexpected properties of special high-altitude, highly-inclined Earth satellite orbits with their apsides in the equator plane.

To verify the results, the orbits have been calculated also in rectangular coordinates with an extended version of the K. Stumpff–E.H. Weiss method (Stumpff and Weiss, 1968a, b).

2. First Order Perturbation Equations for an Oblate Central Body and One or More "Third" Bodies (Model A)

From the Lagrange planetary equations, Cook (1962) has derived expressions for the rates of change of the orbital elements, due to perturbations caused by a third body, under the following simplifying assumptions:

(1) during one revolution of the satellite the third body is not moving, and

(2) the distance of the satellite from the central body is small, compared to the distance of the third body.

From the first assumption, it follows that the semi-major axis is not changing at all, and from the second, that, in the Earth-Moon system, the validity of the model is restricted to orbits with semi-major axes of up to about 7 Earth radii.

In a further step, Cook substituted in the equation for the rate of change of eccentricity the direction cosines, so that it became a function of 15 different angles, which are linear combinations of argument of perigee, longitude of the node and longitude of the perturbing body. Cook stopped here and discussed the possible occurrence of resonance for eccentricity only.

Following Cook's approach and performing for the other orbital elements what he has called "considerable trigonometric manipulation", we get a system of four first order non-linear differential equations for third body perturbations. Adding the terms for the influence of J_2 on $\dot{h}$ and $\dot{g}$, which have been derived by many authors, for example, Orlov (1954), King-Hele (1958), Kozai (1959), yields the formulae as outlined in Table I.

The full model (model A), as presented in Tables I and II, contains 82 terms ($\dot{e}$: 15, $\dot{i}$: 21, $\dot{h}$: 23, $\dot{g}$: 23) per disturbing body plus two terms for the oblate central body.

We notice secular terms in (3) and (4), and, most important, in (1) and (2) sine functions of φ_r only, and in (3) and (4) cosine functions of φ_r only. For $\dot{\varphi}_r = 0$ for

TABLE I

Outline of the first-order perturbation equations for an oblate central body and one or more "third" bodies (model A)

$$\dot{e} = e\sqrt{1-e^2}\,\frac{1}{n}\sum_d K_d \sum_{r=1}^{15} f_{er}(i, i_d)\,\sin\varphi_r \tag{1}$$

$$\dot{i} = \frac{1}{\sqrt{1-e^2}}\,\frac{1}{n}\sum_d K_d \sum_{r=1}^{21} f_{ir}(e^2, i, i_d)\,\sin\varphi_r \tag{2}$$

$$\dot{h} = \frac{1}{\sqrt{1-e^2}}\,\frac{1}{n}\sum_d K_d[f_{h0}(e^2, i, i_d) + \sum_{r=1}^{22} f_{hr}(e^2, i, i_d)\,\cos\varphi_r] - \tag{3}$$

$$\frac{3}{2}\,J_2 n_0 \left(\frac{n}{n_0}\right)^{7/3} \frac{\cos i}{(1-e^2)^2}$$

$$\dot{g} = \sqrt{1-e^2}\,\frac{1}{n}\sum_d K_d[f_{g0}(i, i_d) + \sum_{r=1}^{22} f_{gr}(i, i_d)\,\cos\varphi_r] - \tag{4}$$

$$\frac{1}{\sqrt{1-e^2}}\,\frac{1}{n}\sum_d K_d\,\cos i[f_{h0}(e^2, i, i_d) + \sum_{r=1}^{22} f_{hr}(e^2, i, i_d)\,\cos\varphi_r] +$$

$$\frac{3}{4}\,J_2 n_0 \left(\frac{n}{n_0}\right)^{7/3} \frac{5\,\cos i^2 - 1}{(1-e^2)^2}\,.$$

The following notation is used:

Orbital elements of the satellite		Elements of the disturbing body	
a	semi-major axis	r_d	distance from central body
e	eccentricity	u_d	angle between node and body
i	inclination	i_d	inclination
h	longitude of ascending node	h_d	longitude of ascending node
g	argument of perigee	m_d	mass
n	angular mean motion	n_d	angular mean motion

Other

m_c	mass of central body
R	radius of central body
J_2	2nd zonal harmonic (central body)
$b = h - h_d$	difference of the nodes
$K_d = Gm_d/r_d^3$	constant of disturbing body
$K_d \simeq (m_d/m_c)\,n_d^2$	constant for circular orbit of disturbing body
n_0	angular mean motion of satellite for $a = R$

TABLE II

Details of model A: A list of the 22 angles φ_r* in Equations (1) through (4). The left column contains the angles occurring in the secular and long-periodic terms (models C and D)

φ_r	r	φ_r	r
		$2u_d$	22
$2g$	1	$2g \pm 2u_d$	6,7
b	16	$b \pm 2u_d$	18,19
$2b$	17	$2b \pm 2u_d$	20,21
$b \pm 2g$	2,3	$b \pm 2g \pm 2u_d$	8,9,10,11
$2b \pm 2g$	4,5	$2b \pm 2g \pm 2u_d$	12,13,14,15

one or more r we get, except for special cases, non-zero secular terms for $\dot{e}$ and $\dot{i}$.

3. Simplifications for Restricted Ranges of Orbits (Models B and C) and Circular Orbits (Model D)

If we restrict ourselves in the Earth-Moon-Sun system to orbits with semi-major axes larger than $3R$, the motion of the Moon and the Sun is much faster than the changes of the longitude of the node and of the argument of perigee of the satellite:

$$\dot{u}_{\text{sun}}, \dot{u}_{\text{moon}} \gg \dot{h}, \dot{g}$$

When considering long-term perturbations only, that is, significantly longer than one year, we can average over the mean anomaly of the Moon and of the Sun respectively and ignore all terms containing u_d in the third body perturbation formulae, since these will provide periodic terms at or near double the period of revolution of the disturbing body. We will call this model B. It contains 28 terms $(\dot{e} : 5, \dot{i} : 7, \dot{h} : 8, \dot{g} : 8)$ per disturbing body plus the two terms for the oblate central body. For the Earth-Moon-Sun system we have a total of 58 terms.

When considering very long-term perturbations only, that is, significantly longer than twenty years, we can make a further simplification. Since the Moon's orbit is only slightly inclined to the ecliptic, the longitude of the node of its orbit with respect to the equatorial plane is oscillating by $\pm 13°$ around the direction of equinox, as Cook (1962) already observed. If we average over this oscillation with

* The somewhat irregular assignment of the indices is due to the fact that $\dot{e}$ is not dependent on all φ_r, especially not on b and $2b$

a period of 18.6 y and assume circular orbits of the disturbing bodies, we can merge the perturbations caused by the Moon and the Sun into the formulae for just one single third body. We will call this model C (see appendix A). It contains 28 terms ($\dot{e} : 5, \dot{i} : 7, \dot{h} : 8, \dot{g} : 8$) for Moon and Sun together plus the two terms for the oblateness of the Earth.

For circular orbits ($e = 0$), where $\dot{e} = 0$ and $\dot{g}$ is no longer relevant, model C turns into model D (see appendix B). Model D contains just 5 terms ($\dot{i} : 2, \dot{h} : 3$) for Moon and Sun together plus one term for the oblateness of the Earth.

In the formulae of models C and D we have used the following abbreviations:

$$c_1 = \frac{3}{64} \frac{K_{\text{moon}} + K_{\text{sun}}}{n} \tag{5}$$

$$c_2 = \frac{3}{4} J_2 n_0 \left(\frac{n}{n_0}\right)^{7/3} \tag{6}$$

$$K_{\text{moon}} = \left(\frac{2\pi}{27.3216}\right)^2 \frac{1}{81.45} \quad K_{\text{sun}} = \left(\frac{2\pi}{365.25}\right)^2 .$$

$$J_2 = 0.001083 \quad n_0 = 2\pi\, 17.043$$

One further restriction of all the models must be mentioned. Since the formulae for $\dot{h}$ and $\dot{g}$ contain $\csc(i)$ and $\cot(i)$ as factors, these formulae are not valid at or very near $i = 0°$ and $i = 180°$.

4. "Balanced" Earth Satellite Orbits

For orbits with semi-major axes of about 7 Earth radii, the perturbing effects of the Moon and the Sun and those of the second zonal harmonic of the Earth's field are of equal size, (Roy, 1969). In the region, where the influence of the second harmonic is predominant, that is, for orbits with semi-major axes of up to about 4 Earth radii, the inclinations, where the equilibria of apsides and nodes occur, do not deviate substantially from their values at lower height.

For orbits with a semi-major axis of 7 Earth radii, this property is true only for a restricted range of arguments of perigee ($40° < g < 140°$, $220° < g < 320°$). The left part of Figure 1 gives an example for this range ($g = 90°$ or $270°$).

For orbits with their apsides near or in the equator plane, the curves for the equilibria of the argument of perigee are bending towards $i = 90°$ and are even closing, depending on a and e. The right part of Figure 1 presents this situation for $g = 0°$ or $180°$.

For orbits with $a/R = 7$ and $e < 0.7$ the equilibria of g are closed curves, when the line of apsides is within approximately $\pm 30°$ of the equator plane ($-30° < g < 30°$, $150° < g < 210°$).

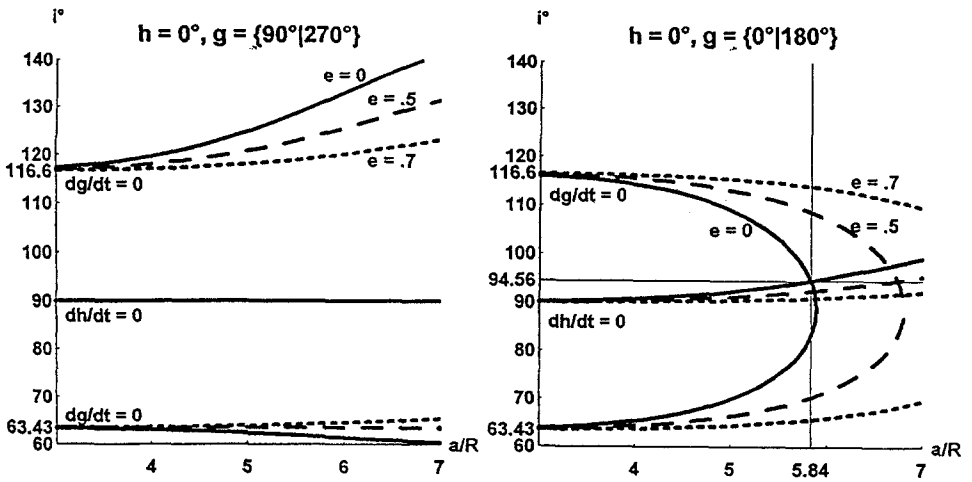

Fig. 1. Secular apsidal and nodal equlibria for the ascending node at vernal equinox ($h = 0°$) and different arguments of perigee (model C).

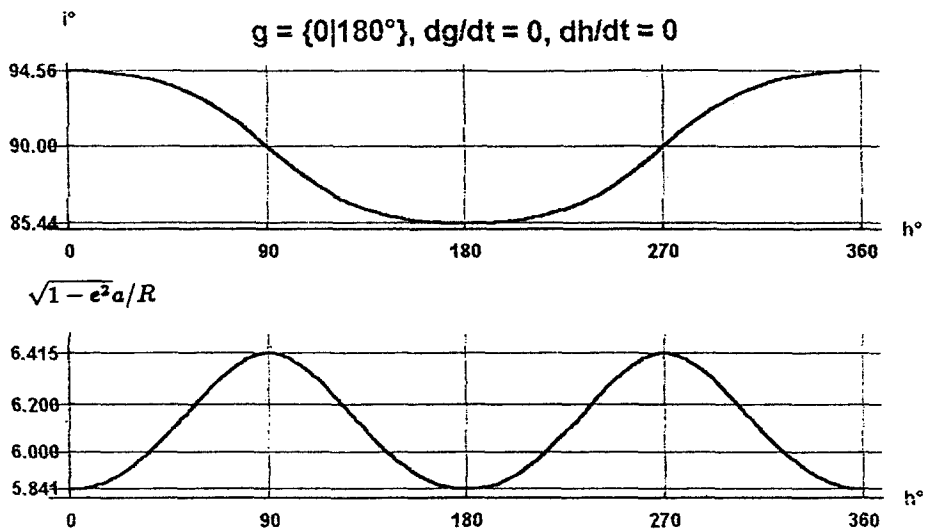

Fig. 2. Inclination, semi-major axis, and eccentricity of simultaneous secular equilibria of apsides and nodes for nodes in the equator plane (model C).

There exist crossing points of the lines for $\dot{g} = 0$ with the lines for $\dot{h} = 0$. While Figure 1 presents the case for the ascending node at vernal equinox ($h = 0°$) only, Figure 2 shows the positions of the crossing points of $\dot{g} = 0$ and $\dot{h} = 0$ for the whole range of nodal positions. Figure 3 shows the secular changes of inclination and eccentricity at these crossing points.

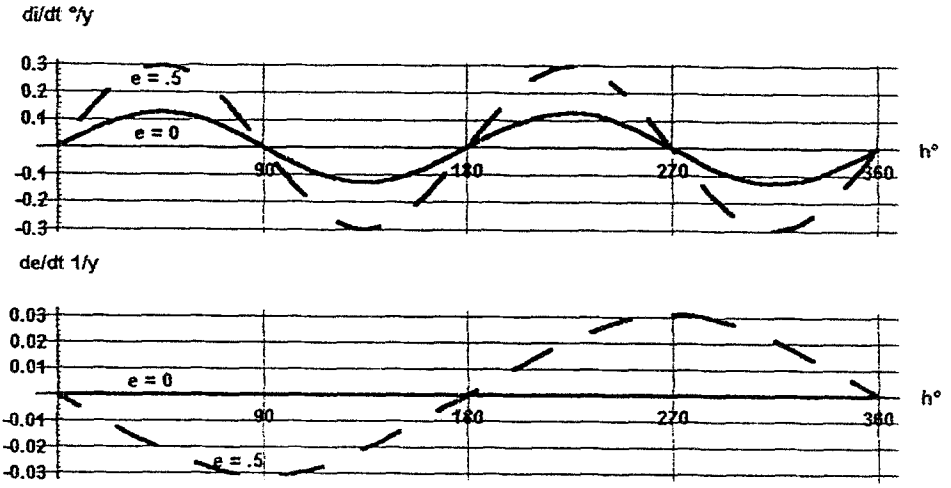

Fig. 3. Secular changes per year of inclination and eccentricity at the simultaneous secular equilibria of apsides and nodes of Figure 2 (model C).

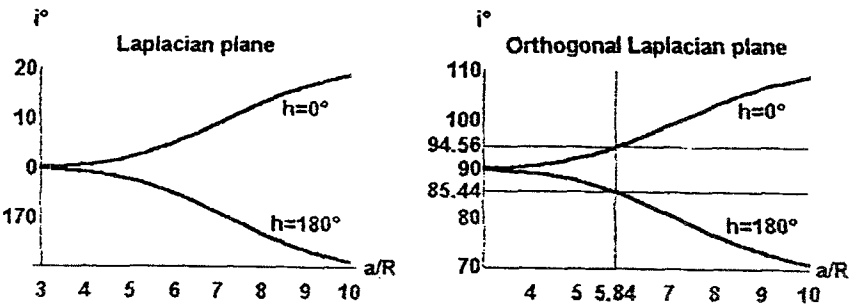

Fig. 4. Equilibria for circular orbits: Prograde and retrograde motion in the Laplacian plane and in the orthogonal Laplacian plane.

From Equations (13) and (14) of model C (see appendix A), we can formulate the following assertions about secular equilibria of eccentricity and inclination, valid within the range of model C:

Assertion 1: *If* $g = j \times 90°$ *and* $b = h - h_d = k \times 180°$ *for* $j, k = 0, 1, 2, 3$ *then* $\dot{e} = \dot{i} = 0$ *independent of e, i, and* i_d.

Assertion 2: *If* $i = 90°$ *and* $g = j \times 90°$ *and* $b = h - h_d = k \times 90°$ *for* $j, k = 0, 1, 2, 3$ *then* $\dot{i} = 0$ *independent of e and* i_d.

Assertion 3: *If* $e = 0$ *then* $\dot{e} = 0$ *independent of b, g, i and* i_d.

In order to find analytical solutions for simultaneous equilibria of e, i, g, and h, we consider, first of all, the cases of Assertion 1. We derive from model C the equations for $h = 90° \mp 90°$ and the four cases where g is a multiple of 90°, that is, $\sin(2g) = 0$. We investigate first the two cases, where $\cos(2g) = +1$, that is, $g = 90° \mp 90°$. When we look for the equilibria conditions $\dot{h} = 0$ and $\dot{g} = 0$, the results are identical for the two values of g and differ in some signs only for the two cases of h ($h = 90° \mp 90°$). The expressions for $\dot{h} = 0$ and $\dot{g} = 0$ can be transformed into explicit equations for η ($\eta = \sqrt{1 - e^2}$):

$$\dot{h} = 0 \rightarrow \eta^5 = -\frac{c_2}{8c_1} \frac{\sin(2i)}{\sin(2(i \mp i_d))} \tag{7}$$

$$\dot{g} = 0 \rightarrow \eta^5 = \frac{c_2}{8c_1} \frac{1 - 5\cos(i)^2}{3 + \sin(i \mp 2i_d)/\sin(i)} . \tag{8}$$

When seeking simultaneous equilibria of h and g, we eliminate η and obtain an implicit equation for the inclination, depending on i_d only:

$$\dot{h} = \dot{g} = 0 \rightarrow (1 - 5\cos(i)^2) \frac{\sin(2(i \mp i_d))}{\sin(2i)} + \frac{\sin(i \mp 2i_d)}{\sin(i)} + 3 = 0 . \tag{9}$$

For $i_d = \varepsilon = 23.44°$, the inclination of the ecliptic, we get two specific solutions for $h = 90° \mp 90°$:

$$i_{r0,1} = 90 \pm 4.56° \tag{10}$$

These two solutions are the retrograde and the prograde motion in the same physical plane. We substitute now the results for the inclination in the equation for η. Since $\sin(2i_{r0})/\sin(2*(i_{r0} - i_d)) = \sin(2i_{r1})/\sin(2*(i_{r1} + i_d))$, the following relation holds for the both cases:

$$\eta \frac{a}{R} = \left(\frac{-\sin(2i_{r0})}{\sin(2(i_{r0} - \varepsilon))} \frac{2J_2 n_0^2}{(K_{\text{moon}} + K_{\text{sun}})} \right)^{1/5} = 5.841 . \tag{11}$$

Equation (9) has two more solutions at $i = \mp 18.08°$, but when we substitute these values in one of the equations for η^5, we get for $\eta \times a/R$ a complex number (fifth root of a negative number). When considering the other two values of g, where $\sin(2g) = 0$ and $\cos(2g) = -1$, that is, $g = 180° \mp 90°$, we get solutions at $i = 90° \mp 61.64°$ and $i = 270° \mp 61.64°$, but for $\eta \times a/R$ also a complex number.

When we search for equilibria of circular orbits – considering Assertion 3 – and since g is no longer relevant, we simply analyse the cases $h = 90° \mp 90°$ and $h = 180° \mp 90°$ of Assertion 1.

For $h = 90° \mp 90°$ we obtain $\dot{h} = 0$

$$-\frac{\sin(2(i \mp i_d))}{\sin(2i)} = \frac{c_2}{8c_1} = \frac{26270}{(a/R)^5} . \tag{12}$$

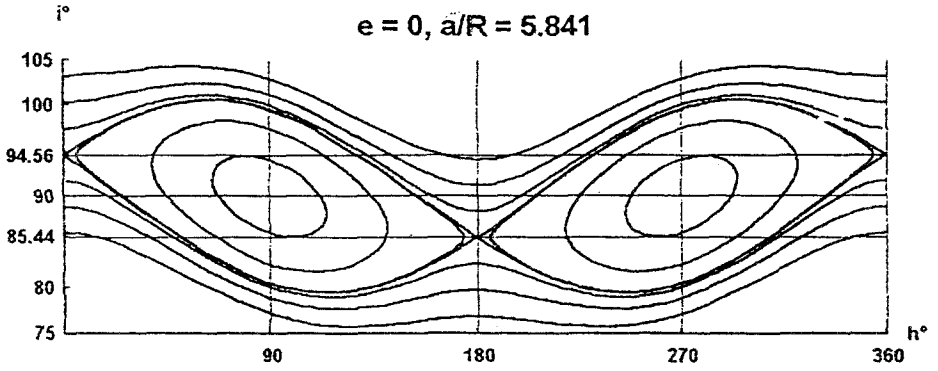

Fig. 5. $i - h$ curves for circular orbits with $a/R = 5.841$. Equations of model D integrated with function "NDSolve" of *Mathematica* (Wolfram, 1988).

TABLE III

Kepler elements of orbits with simultaneous, very long-term equilibria of e, i, g, and h ("Balanced" orbits), derived from model C.

$g = 0°, 180°$					
$e = 0$			$e \neq 0$		
h	i	a/R	h	i	$\sqrt{1-e^2} \times a/R$
90°, 270°	90°	6.415			
0°	94.56°	5.841	0°	94.56°	5.841
180°	85.44°	5.841	180°	85.44°	5.841

Solutions are prograde and retrograde motion in the Laplacian plane, see, for example, Allan and Cook (1964), and prograde and retrograde motion in a plane perpendicular to the Laplacian plane. One instance of the solutions in the plane perpendicular to the Laplacian is the balanced orbit at $a/R = 5.841$ and $i = 94.56°$, see equations (10) and (11).

Considering Assertions 2 and 3, we have all polar, circular orbits ($e = 0$, $i = 90°$) at $h = 180° \mp 90°$ in an equilibrium.

For circular orbits we can draw $i - h$ curves. Figure 5 shows these curves for the near polar region for $a/R = 5.841$. We can see around the equilibria at $i = 90°$ and $h = 180° \mp 90°$ librating orbits up to a separatrix. The hyperbolic points at $i = 90° \pm 4.56°$ and $h = 90° \mp 90°$ are the unstable equilibria of balanced circular orbits.

A summary of the orbits, for which simultaneous equilibria of e, i, g, and h have been found, is shown in Table III.

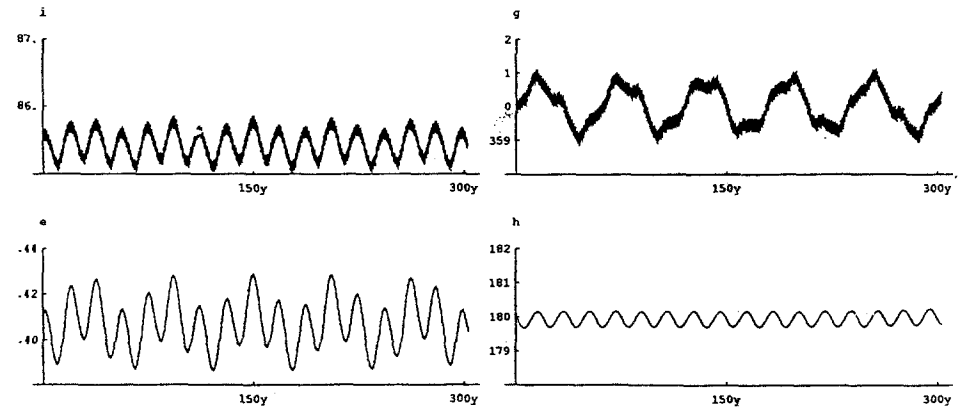

Fig. 6. Variation of Kepler elements of a balanced orbit with a semi-major axis of 6.4087 R and an eccentricity of 0.41147 in the Earth-Satellite-Moon-Sun system over a period of 300 y, corresponding to 1.14×10^5 revolutions. Initial inclination on 1996-04-01 is 94.7139° (model A).

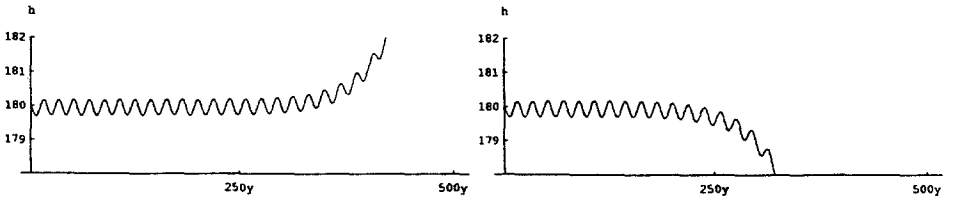

Fig. 7. Variation of the longitude of the node of two orbits with initial inclinations differing by only 1×10^{-4} degrees (model A). The left diagram shows h of the orbit of Figure 6.

5. Comparison of Results With Full Model

We can now compare the predictions of model C, where the inclination of the Moon's orbit to the ecliptic and therefore the motion of the Moon's node is ignored, with the results of model A. Model A treats Moon and Sun separately, but considers circular orbits of the perturbing bodies only. Integration of the system of differential equations of model A is done with the Euler–Cauchy method with intervals of one day. We find orbits at inclinations within a few tenths of a degree of the values predicted by model C, which show a quite regular behaviour over 10^5 orbits or more. Figure 6 presents such an example. The semi-major axis is 6.41 Earth radii, the period is 22.85 hours, and 10^5 orbits correspond to 261 y. The nearly periodic fluctuations of the Kepler elements reflect primarily the motion of the Moon's node. We can see the 18.6 y period perfectly in i and h, whereas in g a period of $3 * 18.6$ y is dominating, and in e both periods are obvious. When looking at Figure 6, we would not expect significant changes in this nearly periodic behaviour.

But after a little more than 300 years the quasi-periodic behaviour is no longer preserved. The left part of Figure 7 shows, for a period of 500 years, the longitude of the node (h) of the example of Figure 6. The right part of Figure 7 shows h of an

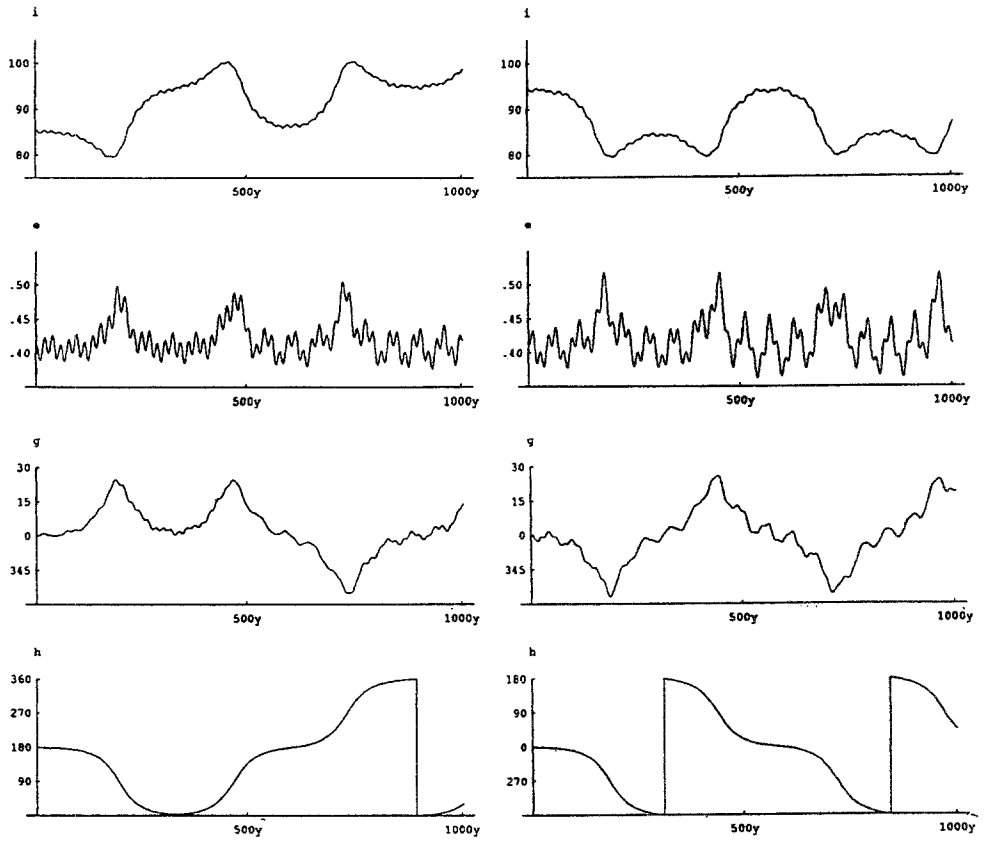

Fig. 8. Variation of Kepler elements of nearly balanced orbits (initial inclination differing by about 0.2 degrees from the unstable equilibrium). Alternate prograde ($h = 180°$, $i = 85.44°$) and retrograde ($h = 0°$, $i = 94.56°$) motion (model A).

orbit with the initial inclination differing by only $1 * 10^{-4}$ degrees from that one to the left. We are confronted with a chaotic behaviour in the immediate vicinity of the equilibrium. A very similar behaviour can be demonstrated also for the retrograde motion.

Extending the evaluation even further, we can see a flip-over of the rotational axis of the orbit to the opposite direction. Figure 8 shows two examples, where the initial inclination differs by about 0.2 degrees from the equilibrium. We can observe the motion of the node, which in one example is librating first and then oscillating, while in the second example oscillation starts immediately.

The described behaviour of orbits near the plane of 94.56° inclination can be demonstrated also with model B and a multi-step integration method ("NDSolve" of *Mathematica*) as well as with a completely different method, described in the next section.

TABLE IV

Initial inclinations for a specific orbit ($a/R = 6.4078$, $e = 0.41147$, $g = 0°$, start date 1996–04–01) where the long-term equilibrium for e, i, h, and g has been found experimentally with different numeric methods and models

	Stumpff–Weiss reference orbit	Model A Euler–Cauchy	Model B NDsolve	Model C
$h = 0°$	94.7191°	94.7138°	94.6075°	94.5596°
$h = 180°$	85.7093°	85.6716°	85.5818°	85.4404°

6. Calculating Perturbations in Rectangular Coordinates (Stumpff – Weiss Method)

The K. Stumpff–E.H. Weiss method (Stumpff and Weiss, 1968a,b) (Stumpff, 1974) handles the n-body problem by solving in suitable intervals $n(n-1)/2$ two-body problems in rectangular coordinates and yields a reference orbit from a weighted linear combination of the two-body results. This approach yields an improvement of two orders of magnitude in precision over the well-known Encke method. Different strategies for controlling the step size have been proposed and compared in the original paper. For the four-body problem of the Earth-Satellite-Moon-Sun system a step size control based on spheres of influence has been implemented. About 50 to 70 steps per one revolution of the satellite yield very reliable results.

The original version of the program did not account for the perturbations by the oblate Earth. An extended version including these perturbations has been implemented.

In order to test the precision of the results, for one specific case ($a/R = 6.4087$, $e = 0.41147$, start date 1996–04–01) the initial inclinations for achieving equilibrium for retrograde and prograde motion have been determined with three methods to a precision of four decimal places:

- an extended version of the Stumpff–Weiss method as described above
- integrating the system of differential equations of model A with the Euler–Cauchy method with stepwidths of one day
- integrating the system of differential equations of model B with the "NDSolve" function of *Mathematica*

The calculations of the ephemerides of the Moon and the Sun for models A and B assume circular orbits of the disturbing bodies (Cook, 1962). The initial ephemerides for the Stumpff–Weiss method are calculated to a much higher precision, as available in popular handbooks (Meeus, 1980), (Montenbruck, 1984). Despite all these differences, the initial inclinations for achieving equilibrium dif-

fer by about only 0.1 degrees. For comparison, the values derived from Model C, which averages over the libration of the Moon's node, differ by a maximum of 0.3 degrees. Table IV lists the actual values of the initial inclinations for achieving equilibrium, as determined by using the different numerical methods.

7. Summary

An analytic model comprising third body perturbations (based on G.E. Cook's first order approach) and the influence of an oblate central body is used in the search for non-standard Earth satellite orbits, suitable for world-wide communications and with minimal or even no station-keeping requirements. Proper simplifications of the equations of motion for a restricted range of a/R yield expressions of reasonable length.

When evaluating special cases, for example orbits with the apsides in the equator plane ($g = 0°$ or $180°$) and at high inclinations, simultaneous secular equilibria of apsides and nodes have been found for $a/R \geq 5.841$. For certain longitudes of the node there exist also secular equilibria of eccentricity and inclination. Orbits, where the secular equilibria of the four Kepler elements e, i, g, and h coincide, have been named "balanced". At $h = 90°$ or $270°$, $i = 90°$, only circular balanced orbits exist. At $h = 0°$, $g = 0°$ or $180°$, $i = 94.56°$, and when $\sqrt{1 - e^2} \times a/R$ equals 5.841, unstable equilibria occur. Near these unstable equilibria, very long-term oscillations between retrograde and prograde motion can be found.

Numeric evaluation of orbits, using the full model or a completely different method (Stumpff–Weiss reference orbits), confirmed the results of the simplified model to within a few tenths of a degree in inclination. Fine-tuning the inclination to within 1×10^{-4} of a degree yields orbits that show only minor fluctuations in their Kepler elements for 10^5 revolutions and more. The fluctuations are caused mainly by the motion of the Moon's node.

Acknowledgements

The author would like to thank E.H. Weiss for providing details of the implementation of the K. Stumpff–E.H. Weiss method, Prof. R. Dvorak of the University of Vienna and his team, especially Mag. E. Lohinger and Ing. E. Vrabec, as well as Prof. Y.V. Batrakov of the Institute for Theoretical Astronomy, St. Petersburg, and Prof. J. Hagel of the Universidade da Madeira for discussions and advice.

Special thanks are due to two anonymous referees who, through their thorough analysis, queries, and suggestions, contributed very much to the structure and the contents of the paper.

Appendix A. Secular and Long-Periodic Perturbations for $3 < a/R < 7$ and $0 < i < \pi$ (Model C)

$$\dot{e} = c_1\, e\sqrt{1-e^2}\,\Big(10(1+3\,\cos(2i_d))\,\sin(i)^2\,\sin(2g)+ \tag{13}$$

$$40\,\sin(i_d)^2\,\cos\left(\frac{i}{2}\right)^4\,\sin(2(b+g))-$$

$$40\,\sin(i_d)^2\,\sin\left(\frac{i}{2}\right)^4\,\sin(2(b-g))-$$

$$40\,\sin(2i_d)\,\cos\left(\frac{i}{2}\right)^2\,\sin(i)\,\sin(b+2g)-$$

$$40\,\sin(2i_d)\,\cos(i)\,\sin\left(\frac{i}{2}\right)^2\,\sin(b-2g)\Big)$$

$$\dot{i} = -c_1\,\frac{1}{\sqrt{1-e^2}}\,\Big(5e^2(1+3\,\cos(2i_d))\,\sin(2i)\,\sin(2g)- \tag{14}$$

$$4(2+3e^2)\,\sin(2i_d)\,\cos(i)\,\sin(b)-$$

$$4(2+3e^2)\,\sin(i_d)^2\,\sin(i)\,\sin(2b)-$$

$$20e^2\,\sin(i_d)^2\,\cos\left(\frac{i}{2}\right)^2\,\sin(i)\,\sin(2(b+g))-$$

$$20e^2\,\sin(i_d)^2\,\sin\left(\frac{i}{2}\right)^2\,\sin(i)\,\sin(2(b-g))-$$

$$10e^2\,\sin(2i_d)\,(\cos(i)-\cos(2i))\,\sin(b-2g)-$$

$$10e^2\,\sin(2i_d)\,(\cos(i)+\cos(2i))\,\sin(b+2g)\Big)$$

$$\dot{h} = c_1\,\frac{\csc(i)}{\sqrt{1-e^2}}\,\Big(-(2+3e^2)\,(1+3\,\cos(2i_d))\,\sin(2i)+ \tag{15}$$

$$5e^2(1+3\,\cos(2i_d))\,\sin(2i)\,\cos(2g)+$$

$$4(2+3e^2)\,\sin(2i_d)\,\cos(2i)\,\cos(b)+$$

$$2(2+3e^2)\,\sin(i_d)^2\,\sin(2i)\,\cos(2b)-$$

$$20e^2 \sin(i_d)^2 \cos\left(\frac{i}{2}\right)^2 \sin(i) \cos(2(b+g))+$$

$$20e^2 \sin(i_d)^2 \sin\left(\frac{i}{2}\right)^2 \sin(i) \cos(2(b-g))-$$

$$10e^2 \sin(2i_d) (\cos(i)+\cos(2i)) \cos(b+2g)+$$

$$10e^2 \sin(2i_d) (\cos(i)-\cos(2i)) \cos(b-2g)\Big) - \frac{2c_2 \cos(i)}{(1-e^2)^2}$$

$$\dot{g} = -c_1 \frac{\cot(i)}{\sqrt{1-e^2}} \Big(-(2+3e^2)(1+3\cos(2i_d)) \sin(2i)+ \tag{16}$$

$$5e^2(1+3\cos(2i_d)) \sin(2i) \cos(2g)+$$

$$4(2+3e^2) \sin(2i_d) \cos(2i) \cos(b)+$$

$$2(2+3e^2) \sin(i_d)^2 \sin(2i) \cos(2b)-$$

$$20e^2 \sin(i_d)^2 \cos\left(\frac{i}{2}\right)^2 \sin(i) \cos(2(b+g))+$$

$$20e^2 \sin(i_d)^2 \sin\left(\frac{i}{2}\right)^2 \sin(i) \cos(2(b-g))-$$

$$10e^2 \sin(2i_d) (\cos(i)+\cos(2i)) \cos(b+2g)+$$

$$10e^2 \sin(2i_d) (\cos(i)-\cos(2i)) \cos(b-2g)\Big)+$$

$$c_1\sqrt{1-e^2} \quad \Big(1+3\cos(2i_d))(1+3\cos(2i))+$$

$$10(1+3\cos(2i_d)) \sin(i)^2 \cos(2g)+$$

$$12 \sin(2i_d) \sin(2i) \cos(b)+$$

$$12 \sin(i_d)^2 \sin(i)^2 \cos(2b)+$$

$$40 \sin(i_d)^2 \cos\left(\frac{i}{2}\right)^4 \cos(2(b+g))+$$

$$40\ \sin(i_d)^2\ \sin\left(\frac{i}{2}\right)^4\ \cos(2(b-g))-$$

$$40\ \sin(2i_d)\ \cos\left(\frac{i}{2}\right)^2\ \sin(i)\ \cos(b+2g)+$$

$$40\ \sin(2i_d)\ \cos(i)\ \sin\left(\frac{i}{2}\right)^2\ \cos(b-2g)\Big) + \frac{c_2\Big(-1+5\ \cos(i)^2\Big)}{(1-e^2)^2}\ .$$

B. Secular and Long-Periodic Perturbations for Circular Orbits (Model D)

$$\dot{i} = -8c_1\ \Big(\sin(2i_d)\ \cos(i)\ \sin(b) - \sin(i_d)^2\ \sin(i)\ \sin(2b)\Big) \tag{17}$$

$$\dot{h} = 2c_1\ \csc(i)\ \Big(-(1+3\ \cos(2i_d))\ \sin(2i)+ \tag{18}$$

$$4\ \sin(2i_d)\ \cos(2i)\ \cos(b) + 2\ \sin(i_d)^2\ \sin(2i)\ \cos(2b)\Big) - 2c_2\ \cos(i)\ .$$

References

Allan, R.R. and Cook, G.E.: 1964, *Proc. R. Soc. Lond.* **A 280**, 97–109.

Cook. G.E.: 1962, *Geophys. J. R. Astr. Soc.* **6**, 271–291.

Hough, M.E.: 1981, *Celest. Mech.* **25**, 111–136.

Hughes, S.: 1980, *Proc. R. Soc. Lond.* **A 372**, 243–264.

King-Hele, D.G.: 1958, *Proc. R. Soc. Lond.* **A 247**, 49–72.

Kozai, Y.: 1959, 'The Earth's Gravitational Potential Derived from the Motion of Satellite 1958 Beta Two', *Smithsonian Inst. Astrophys. Observ. Spec. Rep. 22*, 03/1959, 1–6.

Lidov, M.L.: 1961, *Planet. Space Sci.* **9**, 719–759.

Lidov, M.L.: 1962, 'On the Approximated Analysis of the Orbit Evolution of Artificial Satellites', in *Dynamics of Satellites*, pp. 168–179.

Lorell, J.: 1965, *J. Astronaut. Sci.* **12**, 142–152.

Meeus, J.: 1980, 'Astronomical Formulae for Calculators', *Monografieën over Astronomie en Astrofysica* **4**.

Montenbruck, O.: 1984, 'Grundlagen der Ephemeridenrechnung', *Sterne und Weltraum Taschenbuch* **10**.

Orlov, A.A.: 1954, *Tr. Gos. Astron. Inst. Mosk. Gos. Univ.* **24**, 139–153.

Roy, A.E.: 1969, *Astrophysics and Space Science* **4**, 375–386.

Shapiro, I.I.: 1962, 'The Prediction of Satellite Orbits', in M. Roy (ed.), *Dynamics of Satellites*, pp. 257–312.

Solari G. and Viola R.: 1992, 'M-HEO: The Optimal Satellite System for the Most Highly-Populated Regions of the Northern Hemisphere', *ESA Bull.* **70**, 05/1992, 81–88.

Stumpff, K. and Weiss, E.H.: 1968a, 'A Fast Method of Orbit Computation', *NASA TN D–4470*, 04/1968, 37 p.

Stumpff, K. and Weiss, E.H.: 1968b, 'Application of an N-body Reference Orbit', *The J. Astronaut. Sci.* **XV**, No. 5, pp. 257–261.

Stumpff, K.: 1974, 'Himmelsmechanik', *Vol. III, Chap. XXXI, Sect. 258*, pp. 322–327.

Wolfram, S.: 1988, 'Mathematica: A System for Doing Mathematics by Computer', 2nd ed.